Phase Structure of Dense QCD

Tetsuo HATSUDA

Department of Physics, The University of Tokyo, Tokyo 113-0033, Japan

QCD phase structure and a new critical point at finite baryon density are discussed with special emphasis on the interplay between the dynamical chiral symmetry breaking and the color superconductivity. Results of a model independent Ginzburg-Landau approach and of a phenomenological Nambu–Jona-Lasinio model are presented. A theoretical connection between the hadron-quark phase transtion at finite baryon density and the boson-fermion mixture of ultracold atoms is also discussed.

§1. Introduction

QCD exhibits various phases depending on the temperature T and the baryon chemical potential μ_{B}[1] as illustrated in Fig. 1. Three typical examples are the QGP (quark-gluon plasma) phase at high T, the NG (Nambu-Goldstone) phase at low T and μ_{B}, and the CFL (color-flavor locked) phase at high μ_{B}. Among others, the NG phase is characterized by the dynamical breaking of chiral symmetry due to nonvanishing chiral condensate $\langle\bar{q}q\rangle$.[2] On the other hand, in the color superconductivity at high chemical potential, the diquark condensate $\langle qq\rangle$ is formed.[3] In the presence of these condensates, the light quarks acquire the Dirac type mass M and the Majorana type mass Δ.

Our understanding of the phase structure at finite μ_{B} is still immature due to the severe sign problem in the lattice QCD simulations. Therefore the analyses based on the Ginzburg-Landau (GL) functional and also on effective theories such as the Nambu–Jona-Lasinio (NJL) model are useful to grasp qualitative features of dense QCD. Also, studies on similar many-body systems such as the mixtures of ultracold fermions and bosons may give us a hint to understand dense QCD matter. In the following sections, we will discuss some recent attempts along this line.

§2. Ginzburg-Landau potential for hot/dense QCD

In this section, we focus our attention on the QCD phase structure at intermediate value of the quark chemical potential ($\mu = \mu_{\mathrm{B}}/3 \sim 400$ MeV) where there would be an interplay between the chiral condensate $\langle\bar{q}q\rangle$ and the diquark condensate $\langle qq\rangle$.[4),5] Study of this region is not only important to understand the quantum phase transition to quark matter in the deep interior of the neutron stars, but also interesting in relation to similar phenomena such as the interplay between magnetically ordered phases and metallic superconductivity[6] and that between superfluidity and magnetism in ultracold atoms.[7]

To analyze such interplay in QCD in a model-independent manner, we construct a Ginzburg-Landau (GL) potential Ω on the basis of the QCD symmetry, $\Omega(\Phi, d_{\mathrm{L}}, d_{\mathrm{R}}) = \Omega_{\chi}(\phi) + \Omega_{d}(d_{\mathrm{L}}, d_{\mathrm{R}}) + \Omega_{\chi d}(\Phi, d_{\mathrm{L}}, d_{\mathrm{R}})$. Here the chiral field ϕ, which has

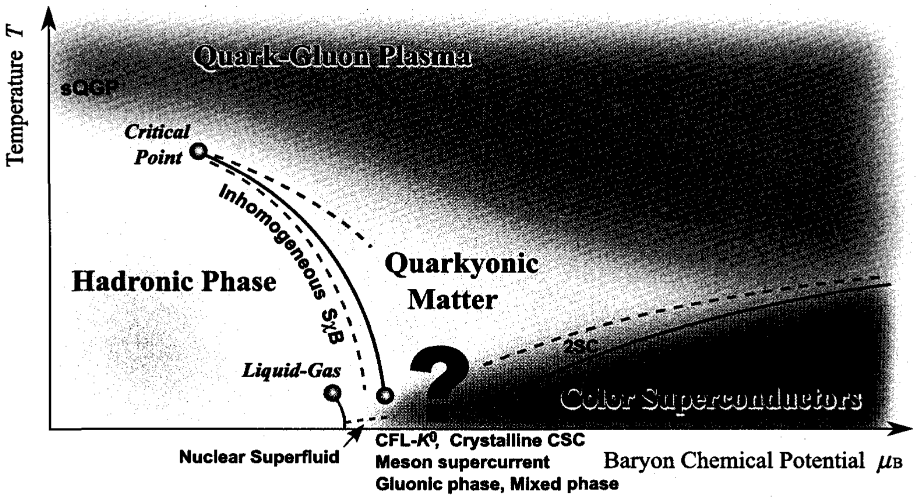

Fig. 1. QCD phase diagram in the plane of temperature T and baryon chemical potential $\mu_{\rm B}$ taken from 1).

a 3×3 matrix structure in the flavor space, is defined by $\phi \equiv \langle \Phi \rangle$ with $\Phi_{ij} \equiv [\bar{q}_{\rm R}]^j_a [q_{\rm L}]^i_a$ having the transformation property, $\phi \to e^{-2i\theta_{\rm A}}\ V_{\rm L}\phi V_{\rm R}^\dagger$. On the other hand, the diquark field $d_{\rm L}$, which has a 3×3 matrix structure in the flavor-color space, is defined by $d_{\rm L} \equiv \langle D_{\rm L} \rangle$ with $[D_{\rm L}^\dagger]_{ai} \equiv \epsilon_{ijk}\epsilon_{abc}[q_{\rm L}]^j_b (i\gamma^2\gamma^0)[q_{\rm L}]^k_c$ having the transformation property, $d_{\rm L} \to e^{2i\theta_{\rm A}} e^{2i\theta_{\rm B}}\ V_{\rm L} d_{\rm L} V_{\rm C}^t$. Similar definition holds for $d_{\rm R}$ too. In the above, $V_{\rm C}$, $V_{\rm L}$, $V_{\rm R}$, $e^{-i\theta_{\rm B}}$ and $e^{-i\theta_{\rm A}}$ belong to $SU(3)_{\rm C}$, $SU(3)_{\rm L}$, $SU(3)_{\rm R}$, $U(1)_{\rm B}$, and $U(1)_{\rm A}$, respectively.

General form of the GL potential in the chiral limit which is invariant under $\mathcal{G} = SU(3)_C \otimes SU(3)_{\rm L} \otimes SU(3)_{\rm R} \otimes U(1)_{\rm B}$, written in terms of the chiral field up to $\mathcal{O}(\phi^4)$, reads,[8)]

$$\Omega_\chi = \frac{a_0}{2}{\rm Tr}\ \phi^\dagger\phi + \frac{b_1}{4!}\left({\rm Tr}\ \phi^\dagger\phi\right)^2 + \frac{b_2}{4!}{\rm Tr}\left(\phi^\dagger\phi\right)^2 - \frac{c_0}{2}\left({\rm det}\phi + {\rm det}\phi^\dagger\right), \qquad (2\cdot1)$$

where "Tr" and "det" are taken over the flavor indices, i and j. The first three terms on the right-hand side are invariant under $\mathcal{G} \otimes U(1)_{\rm A}$, while the last term represents the axial anomaly which breaks $U(1)_{\rm A}$ down to $Z(6)_{\rm A}$. The potential Ω_χ is bounded from below for $b_1 + b_2/3 > 0$ and $b_2 > 0$. If these conditions are not satisfied, we need to introduce terms in $\mathcal{O}(\phi^6)$ to stabilize the potential, a situation we will indeed encounter. We assume c_0 to be positive so that the chiral condensate at low temperature is positive. Also, we assume that a_0 changes its sign at a certain temperature to drive the chiral phase transition. Most general form of the GL potential which is invariant under $\mathcal{G}$, written in terms of the diquark field up to $\mathcal{O}(d^4)$, reads,[9)]

$$\begin{aligned}\Omega_d = \alpha_0\ &{\rm Tr}[d_{\rm L} d_{\rm L}^\dagger + d_{\rm R} d_{\rm R}^\dagger] \\ &+\beta_1\left([{\rm Tr}(d_{\rm L} d_{\rm L}^\dagger)]^2 + [{\rm Tr}(d_{\rm R} d_{\rm R}^\dagger)]^2\right) + \beta_2\left({\rm Tr}[(d_{\rm L} d_{\rm L}^\dagger)^2] + {\rm Tr}[(d_{\rm R} d_{\rm R}^\dagger)^2]\right) \\ &+\beta_3\ {\rm Tr}[(d_{\rm R} d_{\rm L}^\dagger)(d_{\rm L} d_{\rm R}^\dagger)] + \beta_4\ {\rm Tr}(d_{\rm L} d_{\rm L}^\dagger){\rm Tr}(d_{\rm R} d_{\rm R}^\dagger). \qquad (2\cdot2)\end{aligned}$$

The transition from the normal state to color superconductivity is driven by α_0

changing sign. The interaction potential which is invariant under $\mathcal{G}$, written in terms of both chiral and diquark fields to fourth order, reads,[5),10)]

$$\begin{aligned}\Omega_{\chi d} = \gamma_1 \ &\mathrm{Tr}[(d_{\mathrm{R}} d_{\mathrm{L}}^{\dagger})\phi + (d_{\mathrm{L}} d_{\mathrm{R}}^{\dagger})\phi^{\dagger}] \\ &+\lambda_1 \ \mathrm{Tr}[(d_{\mathrm{L}} d_{\mathrm{L}}^{\dagger})\phi\phi^{\dagger} + (d_{\mathrm{R}} d_{\mathrm{R}}^{\dagger})\phi^{\dagger}\phi] + \lambda_2 \ \mathrm{Tr}[d_{\mathrm{L}} d_{\mathrm{L}}^{\dagger} + d_{\mathrm{R}} d_{\mathrm{R}}^{\dagger}] \cdot \mathrm{Tr}[\phi^{\dagger}\phi] \\ &+\lambda_3 \left(\mathrm{det}\phi \cdot \mathrm{Tr}[(d_{\mathrm{L}} d_{\mathrm{R}}^{\dagger})\phi^{-1}] + \mathrm{h.c.}\right). \end{aligned} \tag{2·3}$$

The term with the coefficient γ_1 originates from the axial anomaly which imposes the sign of γ_1 in Eq. (2·3) and that of c_0 in Eq. (2·1) being the same.

Equations (2·1), (2·2) and (2·3) constitute the most general form of the GL potential under the conditions that the phase transition is not strongly first order (i.e., the magnitudes of $\phi, d_{\mathrm{L(R)}}$ are sufficiently smaller than those at zero temperature) and that the condensed phases are spatially homogeneous. To proceed analytically for the flavor-$SU(3)$ chiral limit, we restrict ourselves to maximally symmetric condensates of the form: $\phi = \mathrm{diag}(\sigma,\sigma,\sigma)$, $d_{\mathrm{L}} = -d_{\mathrm{R}} = \mathrm{diag}(d,d,d)$, where σ and d are assumed to be real and spatially uniform. We have chosen the relative sign between d_{L} and d_{R} so that the ground state has positive parity, as is indeed favored by the axial anomaly together with finite quark masses. The above ansatz for the diquark condensate has residual symmetry $SU(3)_{\mathrm{C+L+R}} \otimes Z(2)$ and is called the color-flavor locking (CFL) because of its symmetry realization. (Note that $Z(2)$ corresponds to the reflection, $q_{\mathrm{L(R)}} \to -q_{\mathrm{L(R)}}$.)

The reduced GL potential with the above ansatz reads

$$\Omega_{3\mathrm{F}} = \left(\frac{a}{2}\sigma^2 - \frac{c}{3}\sigma^3 + \frac{b}{4}\sigma^4 + \frac{f}{6}\sigma^6\right) + \left(\frac{\alpha}{2}d^2 + \frac{\beta}{4}d^4\right) - \gamma d^2\sigma + \lambda d^2\sigma^2. \tag{2·4}$$

Here the axial anomaly leads to $c > 0$ and $\gamma > 0$, while microscopic calculation based on the Nambu–Jona-Lasinio model as well as the weak-coupling QCD suggests that λ is positive and plays a minor role in comparison to γ.[10)] Note that we have introduced f-term ($f > 0$) in case that b becomes negative. This system can have four phases with the following dynamical breaking patterns of continuous symmetries;

$$\begin{aligned} \text{QGP phase}: &\ \sigma = 0, d = 0, \\ \text{NG phase}: &\ \sigma \neq 0, d = 0 \ : \ \mathcal{G} \to SU(3)_{\mathrm{C}} \otimes SU(3)_{\mathrm{L+R}} \otimes U(1)_{\mathrm{B}}, \\ \text{CFL phase}: &\ \sigma = 0, d \neq 0 \ : \ \mathcal{G} \to SU(3)_{\mathrm{C+L+R}}, \\ \text{COE phase}: &\ \sigma \neq 0, d \neq 0 \ : \ \mathcal{G} \to SU(3)_{\mathrm{C+L+R}}. \end{aligned} \tag{2·5}$$

The COE (coexistence) phase is favored by the axial anomaly, since the simultaneous presence of d and positive σ makes the GL potential lower because of the γ-term with $\gamma > 0$. Note that even the unbroken discrete symmetry $Z(2)$ is common between CFL and COE phases, so that they cannot be distinguishable from the symmetry point of view. For flavor-$SU(2)$ chiral limit with $m_{\mathrm{u,d}} = 0$ and $m_{\mathrm{s}} = \infty$, the condensates with the s quark disappear, so that we have $\phi = \mathrm{diag}(\sigma,\sigma,0)$ and $d_{\mathrm{L}} = -d_{\mathrm{R}} = \mathrm{diag}(0,0,d)$. Then the reduced GL potential becomes $\Omega_{2\mathrm{F}} = \left(\frac{a}{2}\sigma^2 + \frac{b}{4}\sigma^4 + \frac{f}{6}\sigma^6\right) + \left(\frac{\alpha}{2}d^2 + \frac{\beta}{4}d^4\right) +$

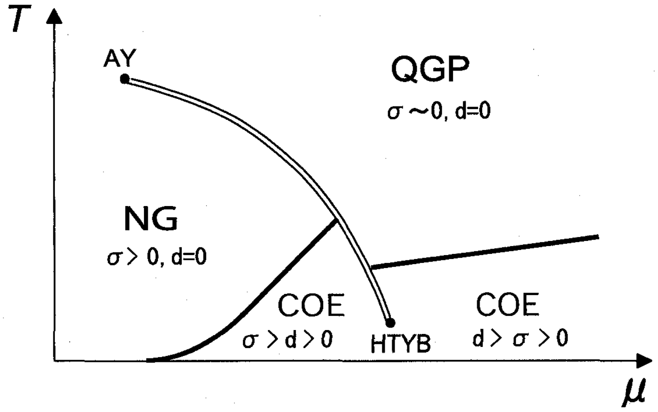

Fig. 2. Schematic phase structure with two light (up and down) quarks and a medium heavy (strange) quark.[5] The double line indicates the first order transition. AY and HTYB are the second-order critical points at which the first-order line terminates.

$\lambda d^2\sigma^2$. Thus, the coexistence of d and σ is disfavored in this case, because of the λ-term with $\lambda > 0$.

The mapping of the phase diagrams obtained from the GL potentials, $\Omega_{3\mathrm{F}}$ and $\Omega_{2\mathrm{F}}$, in the a-α plane to the T-μ plane is a dynamical question which cannot be addressed within the phenomenological GL theory. Nevertheless, we can draw a *speculative* phase structure of QCD for $m_{\mathrm{s}} \sim \Lambda_{\mathrm{QCD}} \gg m_{\mathrm{u,d}} \neq 0$ by interpolating the phase structures obtained from $\Omega_{3\mathrm{F}}$ and $\Omega_{2\mathrm{F}}$ as shown in Fig. 2.[5] In this figure, the double line indicates the first order phase transition driven by the negative b in Eq. (2·4). The single lines indicate the second order phase transitions (within the analysis of the GL potential without fluctuations) which separate the $d \neq 0$ and $d = 0$ phases. We draw two critical points at which the first order phase transition turns into crossover; the one near the vertical axis indicated as "AY" (Asakawa-Yazaki critical point[11]) and the other one near the horizontal axis indicated as "HTYB".[5] The latter is driven by the axial anomaly with positive γ in Eq. (2·4).

The existence of the AY critical point implies that the transition from the NG phase to the QGP phase on the $\mu = 0$ axis is a crossover. Indeed, the lattice QCD Monte Carlo simulations at finite T with the finite-size scaling analyses indicate that the thermal phase transition at $\mu = 0$ is likely to be crossover.[12] On the other hand, the existence of the HTYB critical point implies that the haronic matter (characterized by $\sigma > d > 0$ and the quark matter characterized by $d > \sigma > 0$ are continuously connected with each other and both are classified into the COE phase. This is intimately related to the idea of hadron-quark continuity, i.e. smooth transition from the superfluid/superconducting hadronic matter to the superconducting quark matter.[13),14] Indeed, there are evidences of the continuity not only for the ground state but also for the excitation spectra: Typical example is the continuity of the flavor-octet vector mesons in hadronic matter at low μ and the color-octet gluons in quark matter at high μ.[13),15]

§3. Incorporating the axial anomaly in the NJL model

Let us now try to locate the HTYB critical point in the QCD phase diagram using the phenomenological NJL model.[16] The Lagrangian of the NJL model with three-flavors consists of three terms: $\mathcal{L} = \bar{q}(i\gamma_\mu\partial^\mu - m_q + \mu\gamma_0)q + \mathcal{L}^{(4)} + \mathcal{L}^{(6)}$, where $q = (\mathrm{u}, \mathrm{d}, \mathrm{s})$ is the flavor triplet quark field, m_q is a flavor symmetric quark mass ($m_\mathrm{u} = m_\mathrm{d} = m_\mathrm{s}$), and μ is the quark chemical potential. The four-fermion interaction $\mathcal{L}^{(4)}$ is chosen to have a standard form[2),20)]

$$\mathcal{L}^{(4)} = 8G\mathrm{tr}(\Phi^\dagger\Phi) + 2H\mathrm{tr}[D_\mathrm{L}^\dagger D_\mathrm{L} + D_\mathrm{R}^\dagger D_\mathrm{R}]. \qquad (3\cdot1)$$

The term proportional to G in $\mathcal{L}^{(4)}$ produces attraction of $q\bar{q}$ pairs, leading to the formation of a chiral condensate, while the term proportional to H in $\mathcal{L}^{(4)}$ leads to attraction of qq pairs in the color-anti-triplet and spin-parity $0^\pm$ channel, inducing a color-flavor locked (CFL) condensate. We treat the two couplings G and H as independent parameters.

The six-fermion interaction $\mathcal{L}^{(6)}$ consists of two parts,

$$\mathcal{L}^{(6)} = -8K\left(\det\Phi + \mathrm{h.c.}\right) + K'\left(\mathrm{tr}[(D_\mathrm{R}^\dagger D_\mathrm{L})\Phi] + \mathrm{h.c.}\right). \qquad (3\cdot2)$$

The first part is the standard Kobayashi-Maskawa-'t Hooft (KMT) interaction[21] which breaks $U(1)_A$ symmetry. Consequently the mass of the η' meson becomes larger than that of the other pseudoscalar octet Nambu-Goldstone (NG) bosons (π, η, K) for positive value of K. The second term, as shown in 5), induces a coupling between the chiral and diquark condensates.: It is this term that is responsible for the aforementioned HTYB critical point. We assume $K' > 0$, so that qq pairs in the positive parity channel, $\langle D_\mathrm{L}\rangle = -\langle D_\mathrm{R}\rangle$, are energetically favored. We keep K and K' as independent parameters.

The condensates favored by the interaction $\mathcal{L}^{(4)} + \mathcal{L}^{(6)}$ are the flavor-symmetric chiral and diquark condensates in the spin-parity 0^+ channel, defined by $2\langle\Phi_{ij}\rangle = \chi\delta_{ij}, 2\langle(D_\mathrm{L})_{ai}\rangle = -2\langle(D_\mathrm{R})_{ai}\rangle = s\delta_{ai}$. Here the condensate order parameters are χ and s. The thermodynamic potential of the model at the mean-field level reads[16]

$$\begin{aligned}\Omega(\chi, s; \mu, T) \quad &= \quad U(\chi, s) - \int_{|p|\leq\Lambda} \frac{d^3p}{(2\pi)^3} \sum_\pm \left[8\omega_8^\pm + \omega_1^\pm\right] \\ &\quad -2T\int \frac{d^3p}{(2\pi)^3}\sum_\pm \left[8\ln(1+e^{-\omega_8^\pm/T}) + \ln(1+e^{-\omega_1^\pm/T})\right], \qquad (3\cdot3)\end{aligned}$$

where Λ is a momentum cutoff to regulate the vacuum energy, $U(\chi, s) = 6G\chi^2 + 3H|s|^2 - 4K\chi^3 - \frac{3}{2}K'|s|^2\chi$, is a constant term which is needed to cancel double counting of the interactions, and $\omega_8^\pm = \sqrt{(\sqrt{M^2+p^2} \pm \mu)^2 + (2\Delta)^2}$, $\omega_1^\pm = \sqrt{(\sqrt{M^2+p^2} \pm \mu)^2 + \Delta^2}$ are the dispersion relations for the quasi-quarks in the octet and singlet representations, with M and Δ the dynamical Dirac and Majorana masses, defined by $M = m_q - 4\left(G - \frac{1}{8}K\chi\right)\chi + \frac{1}{4}K'|s|^2$, $\Delta = -2\left(H - \frac{1}{4}K'\chi\right)|s|$.

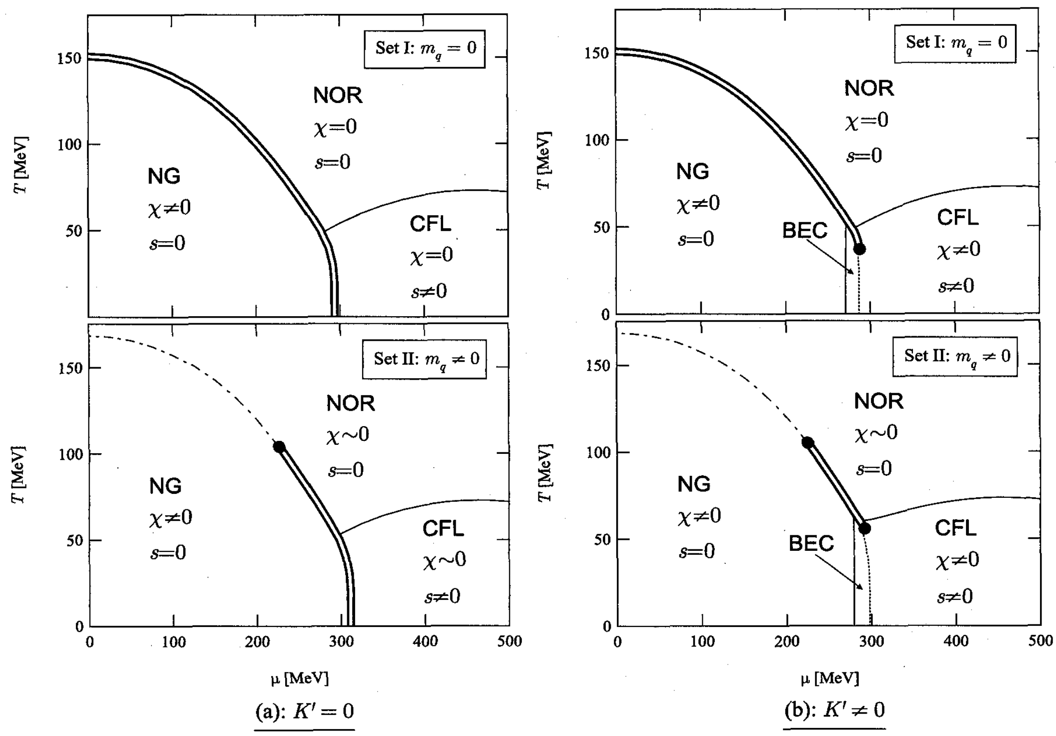

Fig. 3. The phase structure in the (μ, T)-plane in the three-flavor NJL model without (a) and with (b) the K' term. The upper and lower panels present the results in the massless case I and the massive case II respectively. Phase boundaries with a second-order transition are denoted by a single line and a first-order transition by a double line. The dash-dotted line at high T in case II shows the chiral crossover line, while the dotted line in (b) denotes the BEC-BCS crossover. See 16) for further details.

These equations imply that $\chi < 0$ is energetically favored for non-zero m_q, while s is generally complex; the thermodynamic potential is a function of $|s|^2$.

We show in Fig. 3 the phase structures for parameter Set I $(m_q, G\Lambda^2, H\Lambda^2, K\Lambda^5) = (0, 1.926, 1.7, 12.36)$ MeV in the upper panel, and those for Set II $(m_q, G\Lambda^2, H\Lambda^2, K\Lambda^5) = (5.5, 1.918, 1.74, 12.36)$ MeV in the lower panel. Those parameters are taken from 20) with the momentum cutoff $\Lambda = 602.3$ MeV. Panels (a) and (b) show the results without and with the K'-term; in (b) we have taken $K' = 4.2K_0$ with $K_0 = 12.36/\Lambda^5$ as a representative value. The phase diagrams contain a CFL phase with $s \neq 0$ with $U(1)$ baryon number broken, and other two phases both characterized with $s = 0$, a Nambu-Goldstone (NG) phase with $\chi \neq 0$ and a normal (NOR) phase with either $\chi = 0$ (in case $m_q = 0$) or $\chi \sim 0$ (in case $m_q \neq 0$). From the two figures in the panel (a), we see that the current quark mass leads to the AY critical point on the high temperature side of the first-order line of chiral phase transition.[11)] The critical point moves downwards with increasing quark mass m_q since it acts as an external symmetry breaking source of chiral symmetry breaking and thus smears the strength of the phase transition.

The effect of nonvanishing K' can be seen by comparing (a) and (b). We indeed see that the HTYB critical point shows up at the other end of the line of the first order chiral phase transition. This is, as discussed in 5), because the K'-term acts as an external field for χ, which turns the first-order chiral phase transition into a crossover in the CFL phase where $s \neq 0$. Note that the CFL phase in the panel (b) accompanies a nonzero chiral condensate $\chi \neq 0$ induced by the anomaly mixing term in $\mathcal{L}^{(6)}$. The axial anomaly, for sufficiently large chiral-diquark coupling K', not only triggers the HTYB critical point, but also drives a BEC-BCS crossover in the CFL phase, as discussed in 19). Within an NJL-type model such a BEC regime appears for sufficiently large pairing attraction, H, in the qq-channel.[18] The novel feature here is that the axial anomaly helps to realize the BEC regime through its contribution to the effective qq coupling.[16]

The axial anomaly, by driving a coupling between the chiral and diquark condensates, plays an important role in the many body physics of QCD, making the phase diagram extremely rich. For one, we demonstrated that it can indeed produce the low temperature critical point between the hadronic phase and the color superconducting phase predicted by the previous GL analysis.[5] In addition, the coupling helps the formation of a BEC of diquarks via increasing effective quark-quark attraction in the 0^+ channel. As a result, a BEC-BCS crossover or even the a first order BEC-BCS transition can be realized in the CFL phase. We note here that very recently the extension of our analysis incorporating the effect of heavy strange quark mass was reported.[22] It still remains an important task to extend the analyses imposing the charge neutrality and β-equilibrium conditions.

§4. Simulating dense QCD with ultracold atoms

Let us now turn to an intimate correspondence between the ultracold atomic systems and high density QCD matter. Although differing by some twenty orders of magnitude in energy scales, share certain analogous physical aspects, e.g., BEC-BCS crossovers.[19] Motivated by phenomenological studies of QCD that indicate a strong spin-singlet diquark correlation inside the nucleon,[23] we focus here on modeling the transition from the 2-flavor quark matter at high density to the nuclear matter at low density in terms of a boson-fermion system, in which small size diquarks are the bosons, unpaired quarks the fermions, and the extended nucleons are regarded as composite boson-fermion particles.[24] This would be a starting point to understand the quantum phase transition between the hadronic superfluid and the color superconductivity.

Recent advances in atomic physics have made it possible indeed to realize boson-fermion mixture in the laboratory. In particular, tuning the atomic interaction via a Feshbach resonance allows formation of heteronuclear molecules, as recently observed in a mixture of ^{87}Rb and ^{40}K atomic vapors in a 3D optical lattice,[25] and in an optical dipole trap.[26] Let us start from a non-relativistic boson-fermion mixture with Hamiltonian density,

$$
\begin{aligned}
\mathcal{H} = & \frac{1}{2m_\mathrm{b}}|\nabla\varphi(x)|^2 - \mu_\mathrm{b}|\varphi(x)|^2 + \frac{1}{2}\bar{g}_\mathrm{bb}|\varphi(x)|^4 \\
& + \sum_\sigma \left(\frac{1}{2m_\mathrm{f}}|\nabla\psi_\sigma(x)|^2 - \mu_\mathrm{f}|\psi_\sigma(x)|^2 \right) + \bar{g}_\mathrm{ff}|\psi_\uparrow(x)|^2|\psi_\downarrow(x)|^2
\end{aligned}
$$

$$+\sum_{\sigma} \bar{g}_{\rm bf}|\varphi(x)|^2|\psi_\sigma(x)|^2, \tag{4·1}$$

where φ is the boson and ψ the fermion field. The two internal states of the fermions are labeled by spin indices $\sigma = \{\uparrow, \downarrow\}$. For simplicity, we consider an equally populated mixture of n bosons and n fermions with $n_\uparrow = n_\downarrow = n/2$.

The bare boson-fermion coupling $\bar{g}_{\rm bf}$ is related to the renormalized coupling $g_{\rm bf}$ and to the s-wave scattering length $a_{\rm bf}$ by

$$\frac{m_{\rm R}}{2\pi a_{\rm bf}} = \frac{1}{\bar{g}_{\rm bf}} + \int_{|\boldsymbol{k}|\le\Lambda} \frac{d^3k}{(2\pi)^3} \frac{1}{\varepsilon_{\rm b}(k)+\varepsilon_{\rm f}(k)}, \tag{4·2}$$

where $\varepsilon_i(k) = k^2/2m_i$ $(i = {\rm b}, {\rm f})$ is the single-particle kinetic energy, $m_{\rm R}$ is the boson-fermion reduced mass, and $\Lambda = \pi/(2r_0)$ is a high momentum cutoff with r_0 being a typical atomic scale. We assume an attractive bare b-f interaction ($\bar{g}_{\rm bf} < 0$), tunable in magnitude, with Λ fixed, so that the scattering length $a_{\rm bf}$ can change sign: $a_{\rm bf} \to \bar{g}_{\rm bf} m_{\rm R}/(2\pi)$ for small negative $\bar{g}_{\rm bf}$, while $a_{\rm bf} \to r_0$ for large negative $\bar{g}_{\rm bf}$. We keep the bare boson-boson and fermion-fermion interactions fixed and repulsive ($\bar{g}_{\rm bb} > 0, \bar{g}_{\rm ff} > 0$) for the stability of this system.

In the regime of the weak bare b-f coupling where the dimensionless parameter $\eta \equiv -1/(n^{1/3}a_{\rm bf})$ is large and positive, the system at low temperature is a weakly interacting mixture of BEC of the b-bosons (b-BEC) and degenerate f-fermions. The induced interaction through the density fluctuation of b-BEC may also lead to the pairing of f's (f-BCS). On the other hand, in the regime of strong bare b-f coupling where the η is large and negative, bound molecules of b-bosons and f-fermions called *composite fermions*, N = (bf), are formed with a kinetic mass $m_{\rm N} = m_{\rm b} + m_{\rm f}$. The s-wave scattering length of two N's of opposite spins can be estimated by the exchange of constituent b or f,[24]

$$a_{\rm NN} \simeq -\frac{m_{\rm N}}{2m_{\rm R}} a_{\rm bf}. \tag{4·3}$$

This is the same in magnitude but is opposite in sign from the scattering length between difermion molecules due to different statistics. It can be shown that this result is the leading order term in an extension of the present model to large internal degrees of freedom.

Equation (4·3) implies that the low energy effective interaction between composite fermions in the spin-singlet channel is weakly attractive; the stronger the bare b-f attraction the weaker the N-N attraction. Such an effective interaction causes composite fermions to become BCS-paired (N-BCS) below a transition temperature,

$$T_{\rm c}(\text{N-BCS}) = \frac{e^\gamma}{\pi}\left(\frac{2}{e}\right)^{7/3} \varepsilon_{\rm N} e^{\pi/(2k_{\rm F}a_{\rm NN})}. \tag{4·4}$$

where $\varepsilon_{\rm N} = k_{\rm F}^2/2m_{\rm N}$ is the Fermi energy of the N.

The above analyses for large $|\eta|$ suggest a possible phase structures of boson-fermion mixtures in the T-η plane as shown in Fig. 4(a). At intermediate bare b-f

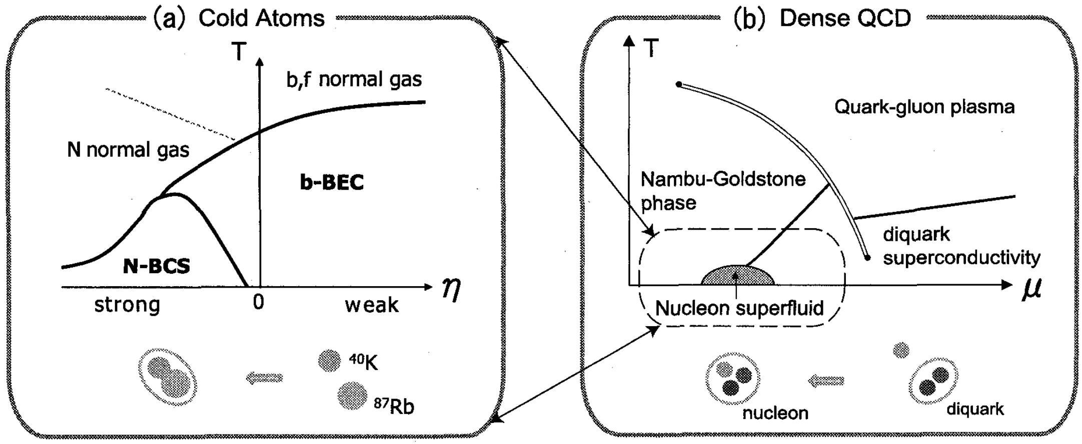

Fig. 4. (a) A possible phase structure of the boson-fermion mixture (such as ^{87}Rb and ^{40}K) in ultracold atoms with attractive b-f interaction and repulsive b-b and f-f interactions. Large and positive (large and negative) η corresponds to the weak (strong) b-f attraction. (b) A possible phase structure of QCD. Large (small) chemical potential μ corresponds to the weak (strong) coupling due to asymptotic freedom.

coupling ($\eta \sim 0$) where a transition from the b-BEC phase to N-BCS takes place, the phase diagram would have complex structure depending on the relative magnitudes of $\bar{g}_{\rm bb}$, $\bar{g}_{\rm ff}$, and $\bar{g}_{\rm bf}$. The f-BCS phase possibly occurs for $\eta > 0$ is not shown in this figure. For more detailed analyses of the phase diagram and its symmetry clasification of the present model, see 24).

The phase structure we find for boson-fermion mixture of ultracold atoms displays features of that in QCD with equal numbers of u and d quarks. The ground state of such system at high density is the 2-flavor color superconductivity (2SC). The order parameter for color-symmetry breaking is the diquark condensate $d_3 = \langle D_3 \rangle$ with the diquark operator $D_c = \epsilon_{ij}\epsilon_{abc}[q]^i_a(i\gamma^2\gamma^0\gamma_5)[q]^j_b$. The gap is of order a few tens of MeV; remaining quarks are unpaired and form degenerate Fermi seas. On the other hand, the ground state of QCD at low density is the nuclear matter with equal numbers of protons and neutrons denoted by $\mathcal{N}^i_{\uparrow,\downarrow}$, a superfluid state with a pairing gap of a few MeV; the order parameter for the spontaneous breaking of baryon-number symmetry $U(1)_{\rm B}$ is the six-quark condensate $\langle \mathcal{N}^i_\uparrow \mathcal{N}^j_\downarrow \rangle = \langle (D_a[q_\uparrow]^i_a)(D_b[q_\downarrow]^j_b) \rangle$. If we model the nucleon, of radius $r_{\mathcal{N}} \sim 0.86$ fm, as a bound molecule of a diquark (of radius $r_d \sim 0.5$ fm) and an unpaired quark, we can make the correspondence between boson-fermion mixture of cold atoms and the diquark-quark mixture. Such correspondence can be also found between the phase diagram of ultracold atoms in Fig. 4(a) and that of dense QCD in Fig. 4(b). In particular, the BCS-like superfluidity of composite fermion (N) with a small gap is a natural consequence of the strong b-f attraction as shown in Eq. (4·3), which may explain why the fermion gap in nucleon superfluidity is order of magnitude smaller than the gap in BEC-like color superconductivity. It is thus quite interesting to carry out the experiments of boson-fermion mixture in ultracold atoms for wide range of the boson-fermion attraction.

Note, however, that tuning the coupling strength at fixed density is not possible in dense QCD matter because of the running coupling $\alpha_{\rm s}(\kappa = \mu)$; furthermore, dynamical breaking of chiral symmetry and its interplay with the color superconductivity have an important role in the quantum phase transition in QCD as discussed in §2. With these reservations in mind, we suggest that fuller understanding, both theoretical and experimental, of the boson-fermion mixture[24] as well as a mixture of three species of atomic fermions[7),27] can reveal properties of high density QCD not readily observable in laboratory experiments.

Acknowledgements

This work was supported by the Grant-in-Aid for Scientific Research (No. 22340052) and in part by the Grant-in-Aid for Scientific Research on Innovative Areas (No. 2004: 20105003). The author thanks H. Abuki, G. Baym, K. Fukushima, M. Tachibana and N. Yamamoto for useful discussions.

References

1) K. Fukushima and T. Hatsuda, arXiv:1005.4814.
2) T. Hatsuda and T. Kunihiro, Phys. Rep. **247** (1994), 221, hep-ph/9401310.
3) M. G. Alford, A. Schmitt, K. Rajagopal and T. Schäfer, Rev. Mod. Phys. **80** (2008), 1455, arXiv:0709.4635.
4) M. Kitazawa, T. Koide, T. Kunihiro and Y. Nemoto, Prog. Theor. Phys. **108** (2002), 929, hep-ph/0207255.
5) T. Hatsuda, M. Tachibana, N. Yamamoto and G. Baym, Phys. Rev. Lett. **97** (2006), 122001, hep-ph/0605018.
6) M. Sigrist and K. Ueda, Rev. Mod. Phys. **63** (1991), 239.
7) R. W. Cherng, G. Refael and E. Demler, Phys. Rev. Lett. **99** (2007), 130406.
8) R. D. Pisarski and F. Wilczek, Phys. Rev. D **29** (1984), 338.
9) K. Iida and G. Baym, Phys. Rev. D **63** (2001), 074018 [Errata; **66** (2002), 059903], hep-ph/0011229.
10) N. Yamamoto, M. Tachibana, T. Hatsuda and G. Baym, Phys. Rev. D **76** (2007), 074001, arXiv:0704.2654.
11) M. Asakawa and K. Yazaki, Nucl. Phys. A **504** (1989), 668.
12) Y. Aoki, G. Endrodi, Z. Fodor, S. D. Katz and K. K. Szabo, Nature **443** (2006), 675, hep-lat/0611014.
13) T. Schafer and F. Wilczek, Phys. Rev. Lett. **82** (1999), 3956, hep-ph/9811473.
14) N. Yamamoto, J. High Energy Phys. **12** (2008), 060, arXiv:0810.2293.
15) T. Hatsuda, M. Tachibana and N. Yamamoto, Phys. Rev. D **78** (2008), 011501, arXiv:0802.4143.
16) H. Abuki, G. Baym, T. Hatsuda and N. Yamamoto, Phys. Rev. D **81** (2010), 125010, arXiv:1003.0408.
17) H. Abuki, T. Hatsuda and K. Itakura, Phys. Rev. D **65** (2002), 074014, hep-ph/0109013.
18) Y. Nishida and H. Abuki, Phys. Rev. D **72** (2005), 096004, hep-ph/0504083.
19) G. Baym, T. Hatsuda, M. Tachibana and N. Yamamoto, J. of Phys. G **35** (2008), 104021, arXiv:0806.2706.
20) M. Buballa, Phys. Rep. **407** (2005), 205, hep-ph/0402234.
21) M. Kobayashi and T. Maskawa, Prog. Theor. Phys. **44** (1970), 1422.
G. 't Hooft, Phys. Rep. **142** (1986), 357.
22) H. Basler and M. Buballa, arXiv:1007.5198.
23) M. Anselmino, E. Predazzi, S. Ekelin, S. Fredriksson and D. B. Lichtenberg, Rev. Mod. Phys. **65** (1993), 1199.
24) K. Maeda, G. Baym and T. Hatsuda, Phys. Rev. Lett. **103** (2009), 085301, arXiv:0904.4372.
25) C. Ospelkaus et al., Phys. Rev. Lett. **97** (2006), 120402.
26) J. J. Zirbel et al. Phys. Rev. A **78** (2008), 013416.
27) A. Rapp, G. Zaránd, C. Honerkamp and W. Hofstetter, Phys. Rev. Lett. **98** (2007), 160405.